

This is the accepted manuscript made available via CHORUS. The article has been published as:

Semiconducting transition-metal oxides based on $d^{\{5\}}$ cations: Theory for MnO and $\text{Fe}_{\{2\}}\text{O}_{\{3\}}$

Haowei Peng and Stephan Lany

Phys. Rev. B **85**, 201202 — Published 17 May 2012

DOI: [10.1103/PhysRevB.85.201202](https://doi.org/10.1103/PhysRevB.85.201202)

Semiconducting transition metal oxides based on d^5 cations: Theory for MnO and Fe_2O_3

Haowei Peng and Stephan Lany*

National Renewable Energy Laboratory, Golden, CO 80401, USA

Transition metal oxides with partially filled d -shells are typically Mott- or charge-transfer insulators with notoriously poor transport properties due to large effective electron/hole masses or due to carrier self-trapping. Employing band-structure calculations and *ab-initio* small-polaron theory for MnO and Fe_2O_3 , we explore the potential of d^5 oxides for achieving desirable semiconducting properties, e.g., in solar energy applications. The quantification of self-trapping energies and the trends with the coordination symmetry suggest strategies to overcome the main bottlenecks, i.e., the tendency for self-trapping of holes due to Mn(II) and of electrons due to Fe(III).

PACS numbers: 71.38.-k, 71.20.Nr, 72.20.-i

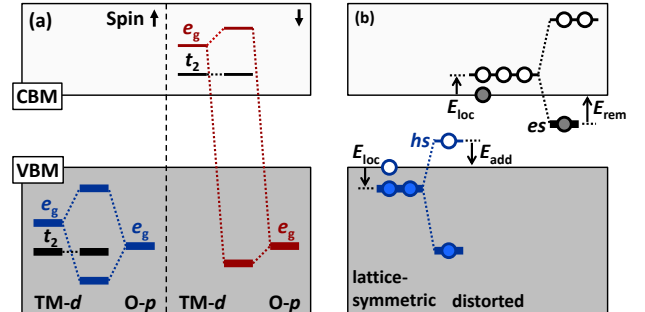
Most transition metal (TM) oxides have a semiconducting band gap and strong optical absorption in the visible range which would make them interesting materials for solar energy conversion, either as photovoltaic or as photo-electro-catalytic absorber materials^{1,2}, for the latter of which oxides are particularly attractive due to their better chemical stability in aqueous environment³. However, efficient charge separation in solar absorbers requires also good carrier transport properties³, which are often deteriorated in TM oxides either by carrier self-trapping that leads to an unfavorable small-polaron transport mechanism⁴⁻⁷, or by high effective masses resulting from narrow d -bands⁸. Hematite Fe_2O_3 has specifically been considered as absorber material for photo-electro-catalytic water splitting³, but its poor majority carrier (electron) mobility resulting from a small-polaron transport mechanism⁹, as well as the very short minority carrier (hole) lifetime, remain barriers for a desirable performance as a photoanode for water-splitting.

Achieving a good hole-mobility and -conductivity is generally difficult in TM oxides, or even in main group oxides^{7,10}. The prototypical p -type oxides are Cu_2O ¹¹ and CuAlO_2 ^{10,12}, where p -type conductivity is facilitated by the p - d repulsion between the O- p and Cu- d ¹⁰ shells^{10,11}. We explore here the prospects of achieving desirable carrier transport properties by means of a d^5 high-spin configuration in TM oxides, where a similar p - d interaction occurs in the occupied spin channel, considering the prototypical Mn(II) and Fe(III) oxides, MnO and Fe_2O_3 . In order to determine band-structure properties, we performed many-body quasi-particle energy calculations in the GW approximation¹³ ("GW" denotes the Greens function G and the screened Coulomb interaction W). In order to determine whether carrier transport occurs in a band- or in a small polaron mechanism, we performed generalized Koopmans calculations^{14,15}, which allow a quantitative evaluation of the carrier self-trapping energy. In addition to the octahedrally coordinated rock-salt (RS) ground state structure of MnO with an antiferromagnetic ordering along the [111] direction, we are considering also the tetrahedrally coordinated zinc-blende (ZB) polymorph¹⁶ with magnetic ordering along the [001]

direction. In hematite Fe_2O_3 , which has an antiferromagnetic double-layer sequence along the c -axis of the hexagonal unit cell¹⁷, the Fe ion is approximately octahedrally coordinated.

As a reference for the following discussion, Fig. 1(a) shows schematically the molecular orbital interactions of a d^5 cation. In octahedral or tetrahedral coordination, the TM d orbitals split into t_2 (d_{xy} , d_{yz} , d_{xz}) and e_g ($d_{x^2-y^2}$, d_{z^2}) crystal field symmetries. In case of the octahedral coordination illustrated in Fig. 1(a), the e_g crystal field state interacts with the same-symmetry state of the oxygen ligands to form bonding and anti-bonding states, whereas the t_2 symmetry is a non-bonding state¹⁸. In tetrahedral coordination (not shown), the coupling scheme is similar, only that the t_2 symmetry is interacting and e_g is non-bonding. Figure 1(b) illustrates the formation of a hole-state or an electron-state inside the gap following the trapping of a carrier into the molecular orbital level that lies closest to the band edge as shown in Fig. 1(a) (see discussion below).

FIG. 1: (a) Schematic illustration of the molecular orbital interactions of a d^5 TM cation (occupied orbital levels are shown bold). (b) Illustration of the formation of a hole state (hs) or an electron state (es) inside the band gap due to the formation of a small polaron.



All electronic structure calculations presented here were performed using the VASP code^{19,20}, and for the computational details we refer to the Supplementary Material²¹ (see, also, references 22–27 therein). As a baseline for subsequent GW¹³ and generalized

Koopmans^{14,15} calculations, we perform density functional calculations using the exchange correlation functional of Ref. 29 in the generalized gradient approximation (GGA) and an onsite Coulomb term²⁵ with $U = 3$ eV for Mn- d and Fe- d . Keeping the GGA+ U wave-functions, the GW energies were iterated to self-consistency, where local field effects derived from the local density functional were taken into account. This procedure yields rather reliable predictions for a range of II-VI and III-V main group compounds³⁰. Metal d -states, however, lie often too high in energy in GW, in both cases of occupied shells, like in ZnO³¹, and unoccupied shells, like in TiO₂ or in V₂O₅³². This problem also accounts for the tendency of common GW approaches to overestimate the band gap of Fe₂O₃ that is formed between occupied O- p and unoccupied Fe- d states³³. As a remedy, we use here an attractive on-site potential for d -states in the form of the non-local external potentials³⁴. By comparison with the experimental band gap energies for MnO (3.4 eV), Mn₃O₄ (2.5 eV), FeO (2.1 eV), and Fe₂O₃ (2.1 eV)³⁵, we find that no such correction is necessary for Mn, but a potential of $V_d = -2.0$ eV is needed for Fe to reconcile experiment and the GW prediction. Our results for RS-MnO are very similar to that of previous GW calculations³⁶.

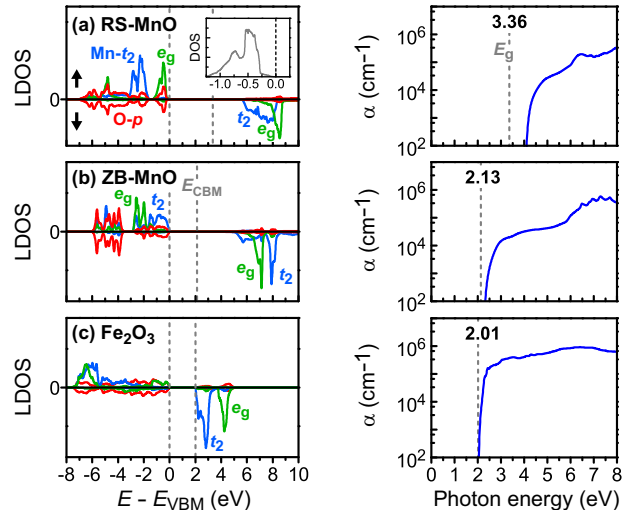
Figure 2 shows the local density of states (LDOS) and the respective absorption spectra for the two polymorphs of MnO and for Fe₂O₃ based on the GW quasi-particle energies. The band-structure features (i.e., the t_2/e_g splitting) anticipated in Fig. 1 are clearly discernible in Fig. 2. Table I gives the GW band gaps and the carrier effective masses. The usual band effective mass is given for electrons in MnO. Due to non-parabolicity and/or anisotropy of the hole masses, and the electron mass in Fe₂O₃, in these cases we give the equivalent effective-mass³² obtained from the integration of the density-of-states weighted with a Boltzmann distribution at 300 K.

TABLE I: Fundamental band gaps (E_g), electron effective masses (m_e^*/m_e), and hole effective masses (m_h^*/m_e) for the two polymorphs of MnO and in Fe₂O₃ from GW calculations²¹.

	E_g (eV)	m_e^*/m_e	m_h^*/m_e
RS-MnO	3.36	0.3	1.2
ZB-MnO	2.13	0.3	4.8
Fe ₂ O ₃	2.01	1.5	2.1

Interestingly, MnO has a highly dispersive s -like conduction band, similar to, say, ZnO, where the unoccupied Mn- d orbitals lie rather far above the conduction band minimum (CBM) [cf. Figs. 2(a) and (b)]. The resulting light effective electron mass suggests excellent electron transport properties in both polymorphs of MnO. The band gap of 2.1 eV in the ZB structure is significantly smaller than the indirect gap of the RS phase, and the overlap of the absorption spectrum with the solar spectrum suggests that MnO could be an interesting solar

FIG. 2: Local density of states and absorption spectrum obtained from many-body GW calculations for (a) MnO in the ground-state rock-salt structure, (b) MnO in the zinc-blende polymorph, and (c) hematite Fe₂O₃. The insert in (a) shows the total density of states in the vicinity of the VBM.



material if the ZB phase can be stabilized. In Fe₂O₃, the CBM is formed by the unoccupied t_2 symmetries of Fe- d [cf. Fig. 2(c)], whose high density of states leads to a very sharp onset of strong optical absorption above the (slightly indirect) band gap, but also causes a relatively heavy electron mass (Table I). Thus, improving the electron transport properties of Fe₂O₃ would require increasing the conduction band dispersion, thereby reducing the large effective mass. This strategy would be also beneficial in view of self-trapping and small-polaron transport for electrons (see below).

Returning to the concept of p - d repulsion as a means to improve hole transport, we now discuss the hole effective masses. The smallest effective hole mass of $m_h^*/m_e = 1.2$ is found for RS-MnO. In this structure, the Mn- d_{z^2} and $d_{x^2-y^2}$ sub-levels of the e_g manifold have lobes pointing directly towards the O ligands, causing a strong p - d interaction [cf. Fig. 1(a)], which leads to a strong valence band dispersion and low DOS in the vicinity of the valence band maximum (VBM) [cf. Fig. 2(a) insert]. In the tetrahedral coordination of Mn in the ZB polymorph, the p - d interaction occurs in the t_2 symmetry. Here, however, the respective Mn- d_{xy} , d_{yz} , and d_{xz} orbitals do not point directly towards the O neighbors (see also below in the context of polarons), leading to a weaker interaction and, hence, to a larger effective mass of $m_h^*/m_e = 4.8$. Similar to Mn in RS-MnO, Fe in Fe₂O₃ is approximately octahedrally coordinated, but the energy of the Fe- d^5 shell lies significantly lower in energy [see Fig. 2(c)], again leading to a weaker p - d interaction than in RS-MnO and a higher mass of $m_h^*/m_e = 2.1$ (see Table I). Nevertheless, all hole masses obtained here are comparable to that of the prototypical p -type oxide Cu₂O ($m_h^*/m_e = 3.7$)³², and still much lower than in many other binary or ternary TM

oxides (the respective calculated values for m_h^*/m_e are 17.0, 10.0 and 18.0 in FeO, CuAlO₂³² and Co₂ZnO₄³⁷, respectively). Thus, the p - d^5 interaction is a promising concept for TM oxides with good hole transport properties.

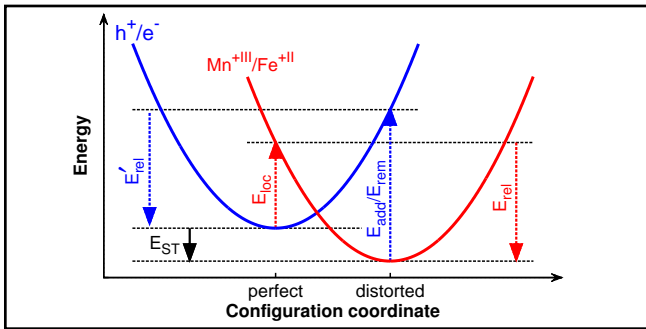
Besides having suitable band-structure properties such as band gap, absorption, and effective masses, a solar absorber material needs further to be robust against carrier *self-trapping*, which not only leads to a small-polaron transport mechanism with notoriously low carrier mobilities³⁸, but also causes deep defect states inside the band gap that can act as effective recombination centers leading to short minority carrier lifetimes. Carrier self-trapping is the result of the localization of an electron or hole at a specific lattice location, forming an electron-state (es) or hole-state (hs) inside the band gap [cf. Fig. 1(b)]. Formally, this process can be described as a change of the oxidation state of the ion at which the electron or hole state is localized, e.g., $\text{Fe}^{+III} + e^- \rightarrow \text{Fe}^{+II}$ ⁹, or $\text{Mn}^{+II} + h^+ \rightarrow \text{Mn}^{+III}$ ⁷ and $\text{O}^{-II} + h^+ \rightarrow \text{O}^{-I}$ ³⁹.

For illustration of the self-trapping process, we plot in Fig. 3 a schematic configuration coordinate diagram. The self-trapping energy

$$E_{ST} = E_{loc} + E_{rel}, \quad (1)$$

can be decomposed⁴⁰ into a localization energy $E_{loc} > 0$ for exciting a carrier from the delocalized band-like state (e^- or h^+) into the respective resonant molecular orbital level [cf. “ E_{loc} ” in Fig. 1(b)], and a relaxation energy $E_{rel} < 0$ which stabilizes the localized polaronic state (e.g., Mn^{+III} or Fe^{+II}).

FIG. 3: The schematic configuration coordinate energy diagram for self-trapping of an excess hole in MnO and an excess electron in Fe₂O₃. h^+ (e^-) denotes a hole (an electron) at the VBM (CBM), whereas Mn^{+III} (Fe^{+II}) denotes the respective self-trapped state.



Theoretical predictions of the self-trapping energy within a first-principles framework have been hampered by the bias of local density (LD) calculations to favor delocalized solutions and the bias of the Hartree-Fock (HF) approach to favor localized solutions⁴¹. Thus, even though the electron-transfer involved in small-polaron hopping in Fe₂O₃ has been studied in great detail using quantum chemical methods⁹, few quantitative pre-

dictions for E_{ST} are presently available^{42,43}. We here employ the density-functional based approach of Ref. 14 and 15 where the delocalization bias is removed by enforcing a generalized Koopmans condition that restores the correct linear variation of the energy with respect to the fractional electron number⁴¹.

In the context of the present polaron calculations, the generalized Koopmans condition states that for a self-trapped hole, the electron addition energy E_{add} should equal the Kohn-Sham single-particle energy of the *initially unoccupied* hole-state, i.e., $E(N+1) - E(N) = e_{hs}(N)$. In order to make this condition satisfied, we introduced in Ref. 14 a parameterized on-site potential

$$V_{hs} = \lambda_{hs}(1 - n_{m,\sigma}/n_{host}) \quad (2)$$

for O- p like hole-states (O^{-I} polarons), where $n_{m,\sigma}$ is the partial charge of the m sublevel of spin σ , n_{host} is the O- p partial charge of the unperturbed host material, and λ_{hs} is a parameter that is adjusted to match the generalized Koopmans condition. For TM- d derived holes states, such as Mn^{+III} in MnO, we apply V_{hs} of the same form as Eq. (2). Since we aim to recover the true quasiparticle energy of the unoccupied hole state relative to the spectrum of the occupied valence band states, we define the reference occupation $n_{host} = 0.94$ by the average Mn- d partial charge of the occupied majority spin direction (“arrow-up” in Fig. 2).

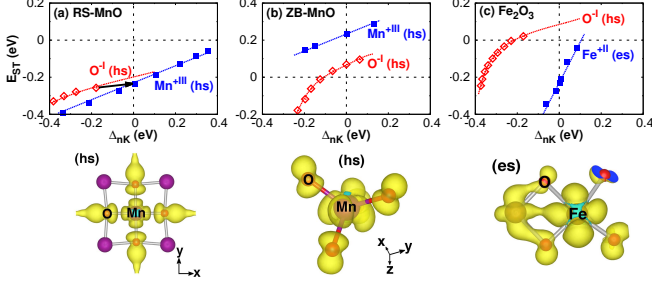
To describe correctly the energy of occupied electron states relative to the spectrum of unoccupied conduction band states, we now define a reference p_{host} that measures the degree to which the d -symmetries that form the CBM are empty, using the definition $p_{m,\sigma} = 1 - n_{m,\sigma}$. The electron state potential analogous to Eq. (2) is then given by

$$V_{es} = \lambda_{es}(p_{m,\sigma}/p_{host} - 1). \quad (3)$$

For the Fe₂O₃, we determine $p_{host} = 0.90$ from the partial charge of the Fe d - t_2 states of the unoccupied minority spin direction which form the CBM [cf. Fig. 2(c)]. The corresponding generalized Koopmans condition for a self-trapped electron is that the electron removal energy E_{rem} should equal the negative single-particle energy of the *initially occupied* electron-state, $E(N-1) - E(N) = -e_{es}(N)$.

The generalized Koopmans calculations were performed using a supercell approach, where the appropriate finite-size corrections for total-energies²⁶ and single-particle energies²⁷ e_{hs} and e_{es} of charged cells have been taken into account (see Supplementary Material²¹). Figure 4 shows the self-trapping energy E_{ST} as a function of the non-Koopmans energy $\Delta_{nK} = E_{add} - e_{hs}$ or $\Delta_{nK} = e_{es} - E_{rem}$, which measures the bias towards delocalization ($\Delta_{nK} > 0$ as in LD) or localization ($\Delta_{nK} < 0$ as in HF). We find that under the correct condition $\Delta_{nK} = 0$, holes self-trap as Mn^{+III} in RS-MnO with a negative $E_{ST} = -0.24$ eV, but not in ZB-MnO where $E_{ST} = +0.23$ eV is positive. Electrons self-trap as Fe^{+II}

FIG. 4: Left panel: the calculated self-trapping energy E_{ST} as a function of the non-Koopmans energy Δ_{nK} , for (a) RS-MnO, (b) ZB-MnO, and (c) Fe_2O_3 . Right panel⁴⁴: Isosurface plot of the squared wave-functions of the Mn^{+III} hole-states in (a) RS-MnO, and in (b) ZB-MnO, and for the Fe^{+II} electron state in (c) Fe_2O_3 .



in Fe_2O_3 with $E_{ST} = -0.23$ eV. The respective parameters in Eq. (2) and Eq. (3) are $\lambda_{hs} = 5.6$ eV, $\lambda_{hs} = 6.5$ eV, and $\lambda_{es} = 0.1$ eV in RS-MnO, ZB-MnO, and Fe_2O_3 respectively [in Fe_2O_3 , GGA+U already satisfies Eq. (3) in good approximation].

We now discuss the physical origin of the carrier self-trapping phenomenology in terms of the decomposition of the self-trapping energy into E_{loc} and E_{rel} [Eq. (1)]. The direct calculation of E_{loc} , which is always positive for self-trapped states⁵, is, however, difficult due to the resonant character of the state inside the continuum of host bands [cf. Fig. 1(b)]. Thus, we determine instead an approximated localization energy E'_{loc} ,

$$E'_{loc} = E_{ST} - E'_{rel} \quad (4)$$

which equals E_{loc} if the energy gain E_{rel} upon lattice distortion following carrier trapping equals the energy gain E'_{rel} upon restoration of the perfect lattice following the carrier-release into the respective band edge (see Fig. 3). (Note that in case of defect bound polarons, where E_{loc} can be negative, it was indeed observed that the two atomic relaxation energies involved in the carrier capture/release cycle are comparable^{14,15,28}.) The result of this analysis is given in Table II.

Addressing the question why self-trapping of Mn^{+III} holes is avoided in ZB-MnO, we observe that: first, E'_{loc} in the RS structure is smaller than in the ZB structure, because the Mn- e_g resonance in RS-MnO peaks closer to VBM [cf. Fig. 2(a)] than the Mn- t_2 resonance in ZB-MnO [cf. Fig. 2(b)]; second, the relaxation energy E'_{rel} stabilizes the polaronic state in the RS structure more than in the ZB structure, which is related to the fact that the Mn- e_g derived hole-state of $d_{x^2-y^2}$ symmetry points directly towards the O ligands [cf. Fig. 4(a)], whereas the Mn- t_2 derived hole-state of d_{xy} symmetry does not [cf. Fig. 4(b)] and therefore interacts less strongly with the ligands. In Fe_2O_3 , the Fe^{+II} electron-state shows a much smaller relaxation energy compared to the Mn^{+III} hole-state, mainly due to the *non-bonding* t_2 character of the electron state [cf. Fig. 1(a)]; the very small localization energy

results from the high Fe- t_2 LDOS at energies just above the CBM [cf. Fig. 2(c)].

TABLE II: The calculated self-trapping energy E_{ST} for the Mn^{+III} hole-states and the Fe^{+II} electron state in MnO and Fe_2O_3 , and the decomposition of E_{ST} into E'_{loc} and E'_{rel} [cf. Eq. (1) and (4)].

Polaron in System	E_{ST} (eV)	E'_{rel} (eV)	E'_{loc} (eV)
Mn^{+III} (hs) in RS-MnO	-0.24	-0.88	+0.64
Mn^{+III} (hs) in ZB-MnO	+0.23	-0.64	+0.87
Fe^{+II} (es) in Fe_2O_3	-0.23	-0.29	+0.06

We further calculated the O^{-I} polarons which were found to be important in TiO_2 ^{8,43}, but we found that E_{ST} is positive in ZB-MnO and Fe_2O_3 , and that the O^{-I} state decays into the Mn^{+III} state in RS-MnO as denoted by the arrow in Fig. 4(a). Considering Mn^{+I} electron-states in MnO and Fe^{+IV} hole states in Fe_2O_3 , we could not identify configurations that could lead to negative self-trapping energies. In view of the fact that the main resonances of the unoccupied Mn- d states in the conduction band and of the occupied Fe- d states in the valence band are separated from the band edge energies by several eV (cf. Fig. 2), we expect rather large localization energies for Mn^{+I} electron states and Fe^{+IV} hole states, which are unlikely to be overcome by the relaxation energy.

Summarizing the results of our calculations, we find that both MnO and Fe_2O_3 have strongly hybridized valence bands due to the p - d^5 coupling, which leads to an increased valence band dispersion and – for a transition metal (TM) oxide – relatively small effective hole masses. The d^5 cations Mn^{+II} and Fe^{+III} exhibit an interesting asymmetry in regard of their carrier trapping behavior: Mn^{+II} tends to trap holes but not electrons, whereas Fe^{+III} tends to trap electrons but not holes. Thus, electrons in MnO and holes in Fe_2O_3 are expected to show band-like transport, but RS-MnO and Fe_2O_3 are predicted to be small-polaron conductors for holes and electrons, respectively. In ZB-MnO, self-trapping is inhibited due to the tetrahedral coordination of Mn. Thus, our study provides specific directions for avoiding the detrimental effects of poor carrier mobility and short minority carrier lifetimes due to self-trapping. In Mn-oxides, hole self-trapping could be avoided by stabilizing the tetrahedral coordination of Mn in ternary oxides or in alloys. In Fe_2O_3 , the quantitative prediction of the self-trapping energy enables approaches for band structure design aiming to lower the CBM energy below the Fe^{+II} electron-trap level whose energy position we have determined here quantitatively. The experimental realization of such d^5 TM oxides with improved transport properties is in progress.

Acknowledgments

This work is supported by the U.S. Department of Energy, Office of Science, Office of Basic Energy Sciences, Energy Frontier Research Centers, under Contract No. DE-AC36-08GO28308 to NREL. The high performance

computing resources of the National Energy Research Scientific Computing Center and of NRELs Computational Science Center are gratefully acknowledged. We thank T.R. Paudel, A. Zunger, A. Zakutayev, N.H. Perry, and T.O. Mason for interest and stimulating discussions on the problem of small-polaron conductivity.

-
- * Electronic address: Stephan.Lany@nrel.gov
- ¹ H. Zhang, G. Chen, and D. W. Bahnemann, *J. Mater. Chem.*, **19**, 5089 (2009).
 - ² C. Wadia, A. P. Alivisatos, D. M. Kammen, *Environ. Sci. Technol.* **43**, 2072 (2009).
 - ³ K. Sivula, F. Le Formal, and M. Graetzel, *Chem. Sus. Chem.* **4**, 432 (2011).
 - ⁴ D. Emin, *Physics Today* **35**, 34 (1982).
 - ⁵ L. D. Landau, *Phys. Z. Sowjet.* **3**, 644 (1933).
 - ⁶ A. M. Stoneham, *J. Chem. Soc., Faraday Trans. 2*, 1989, 85(5), 505-516.
 - ⁷ J. M. Honig, in: *Basic properties of binary oxides*, ed. A. Dominguez-Rodriguez, J. Castaing, and R. Marquez, (University of Seville Press, Seville, 1984), p. 101.
 - ⁸ A. R. Nagaraja, N. H. Perry, T. O. Mason, Y. Tang, M. Grayson, T. R. Paudel, S. Lany, and A. Zunger, *J. Am. Ceram. Soc.* **95**, 269 (2012).
 - ⁹ K. M. Rosso, D. M. A. Smith, and M. Dupuis, *J. Chem. Phys.* **118**, 6455 (2003); N. Iordanova, M. Dupuis, and K. M. Rosso, *J. Chem. Phys.* **122**, 144305 (2005).
 - ¹⁰ H. Kawazoe, M. Yasukawa, H. Hyodo, M. Kurita, H. Yanagi and H. Hosono, *Nature* **389**, 939 (1997).
 - ¹¹ H. Raebiger, S. Lany, and A. Zunger, *Phys. Rev. B* **76**, 045209 (2007).
 - ¹² J. Tate, H. L. Ju, J.C. Moon, A. Zakutayev, A. P. Richard, J. Russell, and D. H. McIntyre, *Phys. Rev. B* **80**, 165206 (2009).
 - ¹³ L. Hedin, *Phys. Rev.* **139**, A796 (1965).
 - ¹⁴ S. Lany and A. Zunger, *Phys. Rev. B* **80**, 085202 (2009).
 - ¹⁵ S. Lany, *Phys. Stat. Sol. (b)* **248**, 1052 (2011).
 - ¹⁶ A. Schrön, C. Rödl, and F. Bechstedt, *Phys. Rev. B* **82**, 165109 (2010).
 - ¹⁷ C. G. Shull, E. O. Wollan, and W. C. Koehler, *Phys. Rev.* **84**, 912 (1951).
 - ¹⁸ Note that in *Oh* symmetry, the six p_m sub-orbitals of the O ligands that point towards the cation site form a_1 , t_1 , and e_g crystal field states, so e_g is the only common representation: J. Osorio-Guillen, S. Lany, S. V. Barabash, and A. Zunger, *Phys. Rev. Lett.* **96**, 107203 (2006); I. S. Elfimov, S. Yunoki, and G. A. Sawatzky, *Phys. Rev. Lett.* **89**, 216403 (2002).
 - ¹⁹ G. Kresse and J. Hafner, *Phys. Rev. B* **47**, 558 (1993); *Phys. Rev. B* **49**, 14251 (1994).
 - ²⁰ M. Shishkin and G. Kresse, *Phys. Rev. B* **74**, 035101 (2006).
 - ²¹ See Supplemental Material at [URL will be inserted by publisher] for details of calculation.
 - ²² P. E. Blöchl, *Phys. Rev. B* **50**, 17953 (1994).
 - ²³ G. Kresse and D. Joubert, *Phys. Rev. B* **59**, 1758 (1999).
 - ²⁴ H. J. Monkhorst and J. D. Pack, *Phys. Rev. B* **13**, 5188 (1976).
 - ²⁵ S. L. Dudarev, G. A. Botton, S. Y. Savrasov, C. J. Humphreys and A. P. Sutton, *Phys. Rev. B* **57**, 1505 (1998).
 - ²⁶ S. Lany and A. Zunger, *Phys. Rev. B* **78**, 235104 (2008).
 - ²⁷ S. Lany and A. Zunger, *Phys. Rev. B* **81**, 113201 (2010).
 - ²⁸ S. Lany and A. Zunger, *Phys. Rev. B* **81**, 205209 (2010).
 - ²⁹ J. P. Perdew, K. Burke, and M. Ernzerhof, *Phys. Rev. Lett.* **77**, 3865 (1996).
 - ³⁰ S. Lany, M. d'Avezac, P. Graf, and A. Zunger, (unpublished).
 - ³¹ M. Shishkin, M. Marsman, and G. Kresse, *Phys. Rev. Lett.* **99**, 246403 (2007).
 - ³² G. Trimarchi, H. Peng, J. Im, A. J. Freeman, V. Cloet, A. Raw, and K. R. Poeppelmeier, K. Biswas, S. Lany, and A. Zunger, *Phys. Rev. B* **84**, 165116 (2011).
 - ³³ P. Liao and E. A. Carter, *Phys. Chem. Chem. Phys.*, **13**, 15189, (2011).
 - ³⁴ S. Lany, H. Raebiger, and A. Zunger, *Phys. Rev. B* **77**, 241201(R) (2008).
 - ³⁵ T. Usani and T. Masumi, *Physica B+C* **86-88**, 985 (1977); H. Y. Xu, S. L. Xu, X. D. Li, H. Wang, and H. Yan, *Appl. Surf. Sci.* **252**, 4091 (2006); H. K. Bowen, D. Adler, and B. H. Auken, *J. Solid State Chem.* **12**, 355 (1975); I. Balberg and H. L. Pinch, *J. Mag. Magn. Mater.* **7**, 12 (1978).
 - ³⁶ S. V. Faleev, M. van Schilfgaarde, and T. Kotani, *Phys. Rev. Lett.* **93**, 126406 (2004); C. Rödl, F. Fuchs, J. Furthmüller, and F. Bechstedt, *Phys. Rev. B* **79**, 235114 (2009).
 - ³⁷ J. D. Perkins, T. R. Paudel, A. Zakutayev, P. F. Ndione, P. A. Parilla, D. L. Young, S. Lany, D. S. Ginley, A. Zunger, N. H. Perry, Y. Tang, M. Grayson, T. O. Mason, J. S. Bettinger, Y. Shi, and M. F. Toney, *Phys. Rev. B* **84**, 205207 (2011).
 - ³⁸ A. J. Bosman and H. J. van Daal, *Adv. Phys.* **19**, 1 (1970).
 - ³⁹ O. F. Schirmer, *J. Phys.: Condens. Matter* **23**, 334218 (2011).
 - ⁴⁰ E. N. Heifets and A. L. Shluger, *J. Phys. Condens. Matter.* **4**, 8311 (1992).
 - ⁴¹ J. P. Perdew et al., *Phys. Rev. A* **76**, 040501(R) (2007).
 - ⁴² D. Munoz Ramo, A. L. Shluger, J. L. Gavartin, and G. Bersuker, *Phys. Rev. Lett.* **99**, 155504 (2007).
 - ⁴³ B. J. Morgan and G. W. Watson, *Phys. Rev. B* **80**, 233102 (2009).
 - ⁴⁴ Figures produced with VESTA: K. Momma and F. Izumi, *J. Appl. Crystallogr.*, **44**, 1272-1276 (2011).